INT. J. REMOTE SENSING, 2001, VOL. 22, NO. 9, 1639–1664

Colour classification of coastal waters of the Ebro river plume from spectral reflectances

F. LAHET, S. OUILLON and P. FORGET

Laboratoire de Sondages Electromagnétiques de l'Environnement Terrestre, Université de Toulon et du Var, BP 132, 83957 La Garde Cedex, France; e-mail: lahet,ouillon,forget@lseet.univ-tln.fr

(*Received 5 May 1999; in final form 22 November 1999*)

Abstract. This paper presents a colour classification of coastal waters from features of spectral reflectance. Experimental data were collected in coastal waters of the Ebro river mouth area during two periods of non-bloom conditions and low suspended load. Examination of the reflectance spectra reveals a few significant shapes corresponding to different apparent colours and specific values of hydrological parameters. A colour classification is proposed. An empirical method and a semi-analytical method are presented in order to retrieve suspended particulate matter concentration, namely *SPM*, chlorophyll a concentration, *chl*, sediment refractive index, m_r, and absorption coefficient of yellow substance at 440 nm, $a_y(440)$. The first method is a direct application of the colour classification. It is based on correlations found for each water type between spectral features of the first derivative of reflectance and *SPM*, *chl*, m_r, $a_y(440)$ values. A second method uses the inversion of a three component reflectance model. Measured reflectance spectra and typical values of m_r, deduced from the colour classification, are assimilated in the model. As a result, it appears that estimates of *SPM* and *chl* are more accurate by calculating *chl* from the correlation technique and *SPM* along with $a_y(440)$ from inversion of the reflectance model.

1. Introduction

Coastal waters are composed of dissolved and particulate matter, both optically active and highly variable in kind and concentration. Consequently, their optical signatures generally show large temporal and spatial variations. In a remote sensing perspective, it may be useful to have some broad information on the optical characteristics of a water without having to specify all the inherent optical properties (IOP). Studies conducted by Jerlov (1951, 1976) in the Baltic Sea led to a classification scheme for marine waters based on the spectral shape of the diffuse attenuation coefficient for downwelling plane irradiance, K_d. The water types are numbered I, IA, IB, II and III for open ocean waters and 1 through 9 for coastal waters. Determining K_d offers many advantages. This quasi-inherent optical property is largely determined by IOPs of the aquatic medium and is not very much altered by changes in the incident radiation field such as a change in solar elevation (Baker and Smith 1979). K_d is routinely measured using the commercially available instruments and does not require absolute measurements. This parameter is of crucial importance in marine biology as its values define the penetration depth of the energy

International Journal of Remote Sensing
ISSN 0143-1161 print/ISSN 1366-5901 online
http://www.tandf.co.uk/journals

available for photosynthesis and are correlated with chlorophyll concentration (Morel 1988). Pelevin and Rutkovskaya (1977) pointed out certain drawbacks of Jerlov's classification, due to experimental limitations at the time of Jerlov's measurements. To overcome this problem, they proposed a classification in terms of K_d(500 nm). They also enlarged the study area, using data from the world ocean. K_d(500 nm) approximately represents the percentage of downwelling light removed, if attenuation is not too intense (Kirk 1994).

These two previous optical classifications are based on the diffuse attenuation coefficient, which is easily measurable but which is not a true IOP of the water. Smith and Baker (1978), on the basis of K_d measurements, observed that attenuation is mainly due to phytoplankton and to its covarying by-products in regions away from terrigenous influences. Since K_d can be directly related to the pigment content, they suggested the classification of such ocean waters from the total chlorophyll-like pigment concentration. Prieur and Sathyendranath (1981) questioned the universality of Jerlov's classification for coastal waters. They showed the important contribution of yellow substance to absorption, in particular in the Baltic Sea and in other coastal waters. This makes Jerlov's classification inapplicable to some regions. Prieur and Sathyendranath (1981) proposed to consider the relative importance of absorption by algal pigments, dissolved organic matter and particulate matter other than phytoplankton. A nomenclature of various water types was proposed from the normalized concentrations of the optically active substances, namely C', Y' and P'. These normalized concentrations can be used to reconstruct the spectral absorption curves. Different waters are classified as C' type, Y' type, P' type or as hybrid types such as $C'P'$, $C'Y'$ or $P'Y'$.

A classification based on the nature of the suspended matter, put forward by Morel and Prieur (1977), has been found useful in the context of remote sensing. 'Case 1' waters are waters in which the concentration of phytoplankton and its derivative products is high compared to that of non-biogenic particles. Therefore absorption by chlorophyll and related pigments plays a major role in determining the total absorption in such waters, although detritus and dissolved organic matter derived from the phytoplankton also contribute to absorption in Case 1 waters. 'Case 2' waters are influenced by phytoplankton, particulate and dissolved organic matter of local and terrigenous origin and mineral particles. Most of the world's sea waters fall into the Case 1 category. Consequently, the pioneer investigations on the applicability of remote sensing in the visible spectrum to study water quality were mainly applied to Case 1 waters. The ratio of reflectances in two bands, e.g. 'blue to green', has been used for a long time (Morel and Prieur 1977) to determine algae chlorophyll concentration. This method has successfully provided large-scale maps of chlorophyll concentration (André and Morel 1991) and the three-dimensional distribution of primary production at local and global scales (Antoine *et al.* 1995).

Nearshore and estuarine Case 2 waters are disproportionately important for human interests as they support different economic activities such as fisheries, fish farming, primary resources exploitation, tourism, etc. These activities induce needs for environmental controls. Case 2 waters have therefore received increasing attention in recent years. However, the use of ocean colour data has been greatly impeded by the difficulty of dealing with their particular and complex optical behaviour. Morel and Gordon (1980) distinguished three approaches for a quantitative use of water colour measurements: analytical, semi-analytical and empirical. The analytical approach is based on the radiative transfer theory. Semi-analytical models consist

of a simplification of the radiative transfer equations aiming, in particular, at reducing computation times. Empirical algorithms are based on the use of reflectance ratios or derivative reflectance spectra.

Generally the use of 'blue to green' ratio for Case 2 waters yields unsatisfactory results as quoted by various authors (Gower *et al.* 1984, Fisher *et al.* 1986, Sathyendranath *et al.* 1989), due to the strong masking effect of absorption by yellow substance and of scattering by suspended particulate matter. Nevertheless the use of reflectance ratios is a way of minimizing overlapping spectral effects of different substances. Statistical relationships based on reflectance ratios were established to retrieve sediment and chlorophyll concentrations (Carder *et al.* 1991, Tassan 1998). The influence of yellow substance was considerably reduced. However the inversion algorithms using reflectance ratios rely on the assumption that the effects of environmental variability are either small or can be considered as spectrally additive constants independent of wavelength.

When these assumptions do not hold, derivative spectra can be used to eliminate background signals and to resolve overlapping spectral features. Many applications of this method can be anticipated. Chen *et al.* (1992) measured reflectance and suspended sediment concentration in laboratory and in north-east of England coastal waters. Their results indicated that reflectance first derivatives at 560 and 727 nm are strongly correlated with the suspended sediment concentration. On the basis of laboratory experiments, Goodin *et al.* (1993) showed that reflectance first derivative at 720 nm is correlated with the sediment concentration and the difference between the second derivatives at 660 and 695 nm with the chlorophyll concentration. Rundquist *et al.* (1996) conducted experiments in a water tank by varying the algal chlorophyll concentration. The use of the ratio of near-infrared (NIR, 705 nm) to red (670 nm) reflectance appears well suited for low chlorophyll concentrations over a narrow range and the first derivative of reflectance at 690.7 nm is better for high chlorophyll concentrations over a wide range. Han and Rundquist (1997) collected similar data in a turbid reservoir. Their results indicated that the first derivative of reflectance is better correlated with chlorophyll concentration than the NIR/red band ratio. Fraser (1998) conducted a study among 22 fresh to alkaline lakes in Nebraska. He observed a significant correlation between the first derivatives at 429, 628 and 695 nm and turbidity. Chlorophyll a content is correlated with first derivatives at 429 and 695 nm.

In this paper, an empirical method and a semi-analytical method will be proposed in order to estimate water quality parameters. The experimental data used have been collected in the framework of the FANS Program (Fluxes Across Narrow Shelves, MAST3, European Community). The general aim of the FANS Program is to improve the knowledge of water fluxes and associated sediment and nutrient fluxes in narrow shelves. The study area is the Ebro delta, on the north-eastern coast of Spain. An integrated approach including *in situ* data, satellite imagery and modelling has been carried out at LSEET to study the suspended matter dispersion (Durand *et al.* 2000). A spectrometer was acquired and a reflectance model was developed in order to characterize the water masses from visible remote sensing.

We propose a colour classification dealing with the determination of water quality parameters in coastal waters. Both advantages of using an optical classification and determining water quality parameters from first derivative reflectance spectra are combined. Examination of a collection of reflectance spectra measured in the Ebro river plume reveals a few significant shapes corresponding to different apparent

water colours (brownish-green, green, blue-green, blue). Each water type is associated with typical values of hydrological data. In the first section, we describe the field measurements. The characterization of the water types from inversion of a reflectance model in terms of m_r, $a_y(440)$ is presented in §3. A colour classification is then proposed in §4. Finally the retrieval of suspended particulate matter concentration and chlorophyll concentration, from inversion of a reflectance model partly parametrized thanks to the colour classification, is addressed in §5.

2. Field measurements

2.1. *Study area*

The Ebro river is the main Spanish river flowing into the Mediterranean Sea. The river is 928 km long with a drainage basin extending 85 835 km^2. Its mean annual flow rate is only 385 $m^3 s^{-1}$ and the flow regime is irregular. Maximum water discharge ($>900\,m^3 s^{-1}$) takes place during spring and autumn, while minimum water discharge ($<200\,m^3 s^{-1}$) occurs mainly during summer. The river has developed a delta of about 320 km^2 located at 40°40′ N and 0°40′ E. The tide amplitude along the coast is low, about 20 cm (Ibañez *et al.* 1997).

In recent centuries, this fluvial system has been greatly affected by human activities (Guillén and Palanques 1992). Many dams and reservoirs were built in the twentieth century. Dams have a major effect on the composition of the suspended sediments (Palanques *et al.* 1990). They trap a high proportion of the suspended load transported by the river. The decreasing current strength causes the particles with the highest settling velocity, such as sand, to settle. The mineral particles that are capable of passing across the dams are more likely to be particles of low sedimentation velocity, such as clay minerals. A mud deposit, between water depths of 20 m and 80–90 m, surrounds the deltaic front and extends southward parallel to the coast. The sediment consists of 60–70% clay and of 30–40% silt. At the edges of the mud belt the grain size increases (on average, 40% clay, 45% silt, 10% sand).

Palanques and Drake (1990) studied the concentration, distribution and sediment dynamics of the SPM. Sampling cruises were carried out in October 1984, April 1985 and May 1986. SPM concentration in the surface waters ranged from less than 0.1 $mg l^{-1}$ to about 1 $mg l^{-1}$. Guillén and Palanques (1992) measured SPM concentrations around 4 $mg l^{-1}$ at the river mouth during seven field campaigns between May 1988 and February 1990. Duarte *et al.* (1998) realized a two-year time series of measurements (March 1992–March 1994) in the Bay of Blanes, located 170 km north of the river mouth. Chlorophyll a concentrations were generally less than 1 $\mu g l^{-1}$ with a maximum value of 5.7 $\mu g l^{-1}$ (March 1992). Phytoplankton blooms were generally observed in late winter (early March) and summer (July). Concerning the algal species, Mura *et al.* (1996) observed that the phytoplankton community in the Bay of Blanes was dominated by diatoms.

2.2. *Field data*

Experimental data were collected during two field campaigns from 29 October to 9 November 1996 (Fliper 1—FLuxes Induced by the Plume of Ebro River) and from 28 June to 8 July 1997 (Fliper3). These periods generally correspond to non-bloom conditions (Duarte *et al.* 1998). They consisted of CTD (Conductivity-Temperature-Depth) profiles, water sampling and reflectance spectra measurements. Water sampling was performed most of the time according to a quasi-Lagrangian sampling strategy, following a surface drifter. The sampling station positions are

shown on figure 1. Five to ten water samples were collected at each station depending on the local stratification as indicated by the CTD profiles and on the station location, inside or outside the plume. A weighted polystyrene floating plate connected to the vessel with 7 m long Teflon tubes allowed sampling to be beyond the influence of the ship (Naudin *et al.* 1997). The water samples were immediately filtered and then analysed on return.

Suspended particulate matter concentrations were determined gravimetrically at Arago Laboratory (Banyuls-sur-Mer, France). Double and triple weighings of the filters produce maximum variations of $\pm 2\%$ but fluctuations were found to be higher when $C < 1\,\mathrm{mg\,l^{-1}}$. We consider an experimental uncertainty, $\Delta(SPM_{\mathrm{exp}})$, equal to $\pm 5\%$ for the whole samples. Chlorophyll a, b and c concentrations were measured in duplo with a spectrophotometer at the Centre d'Estudis Avancats de Blanes. The precision of the spectrophotometric method for the determination of chlorophyll a concentration $\Delta(chl_{\mathrm{exp}})$, is about $\pm 0.125\,\mu\mathrm{g\,l^{-1}}$ when chl_{exp} is of the order of $5\,\mu\mathrm{g\,l^{-1}}$. Only the near surface samples (25 cm depth) were considered in the frame of our study as reflectance measurements were done above the water

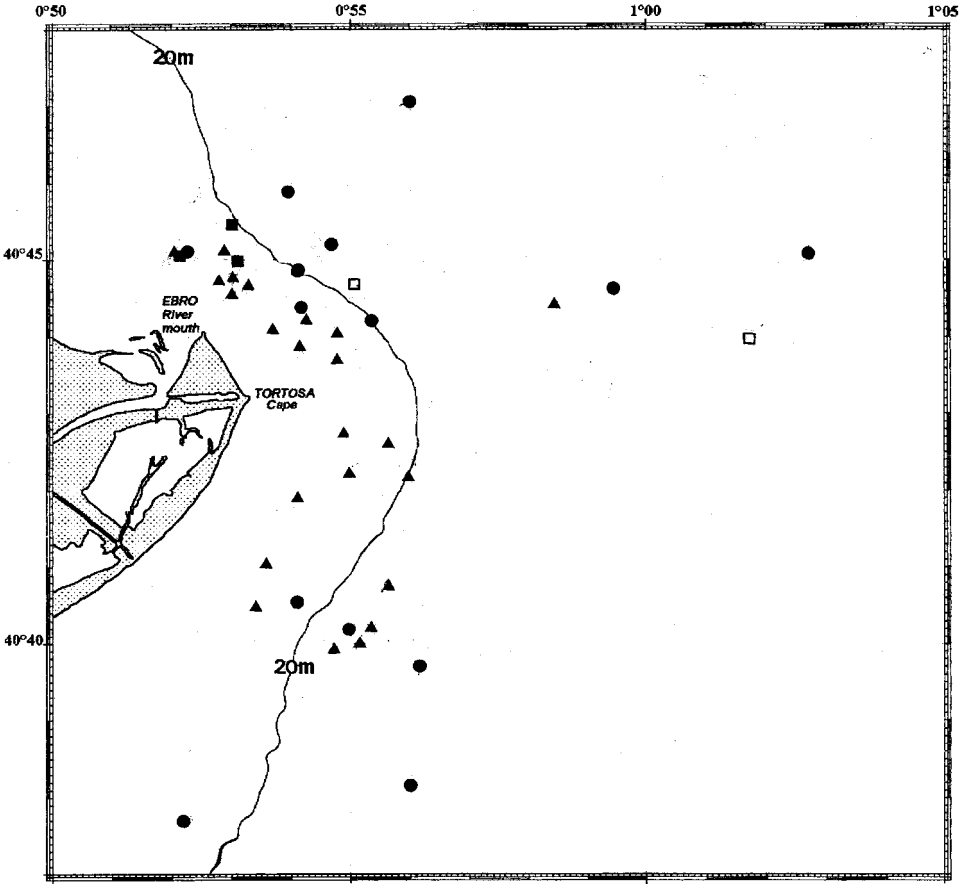

Figure 1. Position of the sampling stations for the two field campaigns (29 October–9 November 1996 and 28 June–8 July 1997) and associated water mass classes. BrG waters, black squares; Gr waters, black triangles; BlG waters, black circles; Bl waters, white squares.

surface. A dataset of 29 (Fliper1) and 32 (Fliper3) coincident radiometric and water parameter measurements are available for the two campaigns.

2.3. *Reflectance measurements*

Reflectance spectra were measured with a PC1000 Ocean Optics spectrometer in the range 400–900 nm with an optical resolution of 10 nm. This optical instrument was operated above the water surface, from the deck of a boat. The collector for irradiance measurements was a cosine collector of opaline glass diffusing material. This sensor was mounted on a perch, located a few metres from the boat and placed so as to avoid ship shadowing effects. E_d and E_u were measured by pointing the perch respectively upwards (directed towards the sky) and downwards (directed towards the sea), the sensor being orientated normally to the sea surface. All the measurements were done in conditions of clear and uncloudy sky and of smooth sea without foam. The irradiance ratio is calculated by averaging two to four consecutive spectra of E_d and E_u. The values are considered in the range 400–800 nm as they can be too noisy between 800 and 900 nm. Then the ratio is converted into subsurface reflectance after removal of surface effects (Forget and Ouillon 1998).

3. Reflectance model and inversion procedure

A three-component reflectance model that takes into account the contributions of dissolved organic matter, phytoplankton and mineral particles was developed. The principle of inversion of the model, in terms of sediment refractive index, m_r, and absorption coefficient of yellow substance at 440 nm, $a_y(440)$, is addressed in Forget *et al.* (1999) in the case of non-chlorophyllous turbid coastal waters. The optical effect of phytoplankton is taken into account in Lahet *et al.* (2000) to make the reflectance model suitable for a broader variety of coastal waters. The bottom is mainly composed of sand between the 10 and 20 m isobaths and of mud beyond the 20 m isobath. Spitzer and Dirks (1987) measured the irradiance reflectance spectra of water with sand-type and mud-type bottoms, at the bottom and 1, 2, 5, 10 and 20 m above. If we consider the values at 10 m depth, the reflectance of the sand-type bottom and the reflectance of mud-type bottom are less than 0.02. In our experiments, the reflectance measurements were carried out on stations with water depths greater than 15 m. We will then assume that bottom effects can be neglected.

The main equations of the reflectance model are summarized hereafter. Spectral light absorption and backscattering coefficients are two IOPs directly ruling the diffuse reflectance, R, of the ocean. The classical model of Gordon *et al.* (1975) is considered:

$$R(\lambda) \simeq 0.33 \frac{b_b(\lambda)}{a(\lambda)+b_b(\lambda)} \tag{1}$$

where a and b_b are respectively the absorption and backscattering coefficients of the water body. Coefficients a and b_b are expressed as the sum of contributions from optically active constituents:

$$a(\lambda)=a_w(\lambda)+a_y(\lambda)+a_{ph}(\lambda) \tag{2}$$

$$b_b(\lambda)=b_{bw}(\lambda)+b_{bs}(\lambda)+b_{bph}(\lambda) \tag{3}$$

where subscripts w, y, ph and s stand for water, yellow substance, phytoplankton and sediment respectively. Values of $a_w(\lambda)$ are taken from Pope and Fry (1997).

Absorption by yellow substance is assumed to increase exponentially with decreasing wavelength from visible to ultraviolet (e.g. Bricaud *et al.* 1981) and can be modelled in coastal waters by (Carder *et al.* 1991, Blough *et al.* 1993):

$$a_y(\lambda)=a_y(\lambda_0)\exp[-0.014(\lambda-\lambda_0)] \tag{4}$$

with wavelengths expressed in nanometers. λ_0 is a reference wavelength in the blue part of the spectrum, taken to be equal to 440 nm. In this study, we assume that absorption by biogenic matter only originates from living pigmented algal cells. a_{ph} is calculated from the chlorophyll a specific absorption coefficient of living phytoplankton, $a^*_{ph}(\lambda)$, parametrized by Bricaud *et al.* (1995):

$$a_{ph}(\lambda)=a^*_{ph}(\lambda)\,chl \tag{5}$$

This relation can be used in Case 2 waters because of the additive property of the total absorption coefficient.

b_{bw} is taken to equal one-half of the total scattering coefficient of water, whose values are taken from Smith and Baker (1981). We model light scattering by suspended particles using Mie theory (Van de Hulst 1957) which allows us to express $b_{bs}(\lambda)$ by (Forget *et al.* 1999):

$$b_{bs}(\lambda)=\frac{3C}{2\rho_s \ln\left(\frac{D_{min}}{D_{max}}\right)}\int_{D_{min}}^{D_{max}} Q_{bb}(D,m_r,\lambda)D^{-2}\,dD \tag{6}$$

where ρ_s is the sediment density, D the diameter of sediment particles and Q_{bb} the backscattering efficiency factor of sediment particles of refractive index m_r. A Junge particle size distribution of slope -4 has been assumed in equation (6). The range of particle sizes is $(D_{min}, D_{max})=0.1-100\,\mu$m. As we have no information on the algal species of the Ebro river plume, the contribution of phytoplankton, b_{bph}, is calculated from a mean value of the chlorophyll a specific backscattering coefficient, b^*_{bph}, measured for nine species of phytoplankton (Ahn *et al.* 1992):

$$b_{bph}(\lambda)=b^*_{bph}(\lambda)\,chl \tag{7}$$

Inputs in the model are chlorophyll a concentration and suspended particulate matter concentration. The inversion procedure consists of minimizing the quadratic difference, G, between measured reflectance values, $R_{exp}(\lambda)$, and modelled reflectance values, $R_{mod}(\lambda)$, calculated by varying the values of m_r and $a_y(440)$.

$$G(m_r,a_y(440))=\sum_{\lambda}[R_{mod}(\lambda)-R_{exp}(\lambda)]^2 \tag{8}$$

4. Colour classification

4.1. *Identification of water classes*

The reflectance spectra collected in the Ebro river mouth area are classified according to the value of the wavelength at which the reflectance is maximum, λ_{max}, and which determines the 'colour' of the water. This colour is induced by the nature and the quantity of the main optically active constituents. Photosynthetic pigments, dominated by chlorophyll a, induce a relatively high specific absorption coefficient of the autotrophic planktonic communities in the blue and red bands (Kirk 1994). In contrast, the absorption spectra of inorganic particles (Kirk 1994), detritus

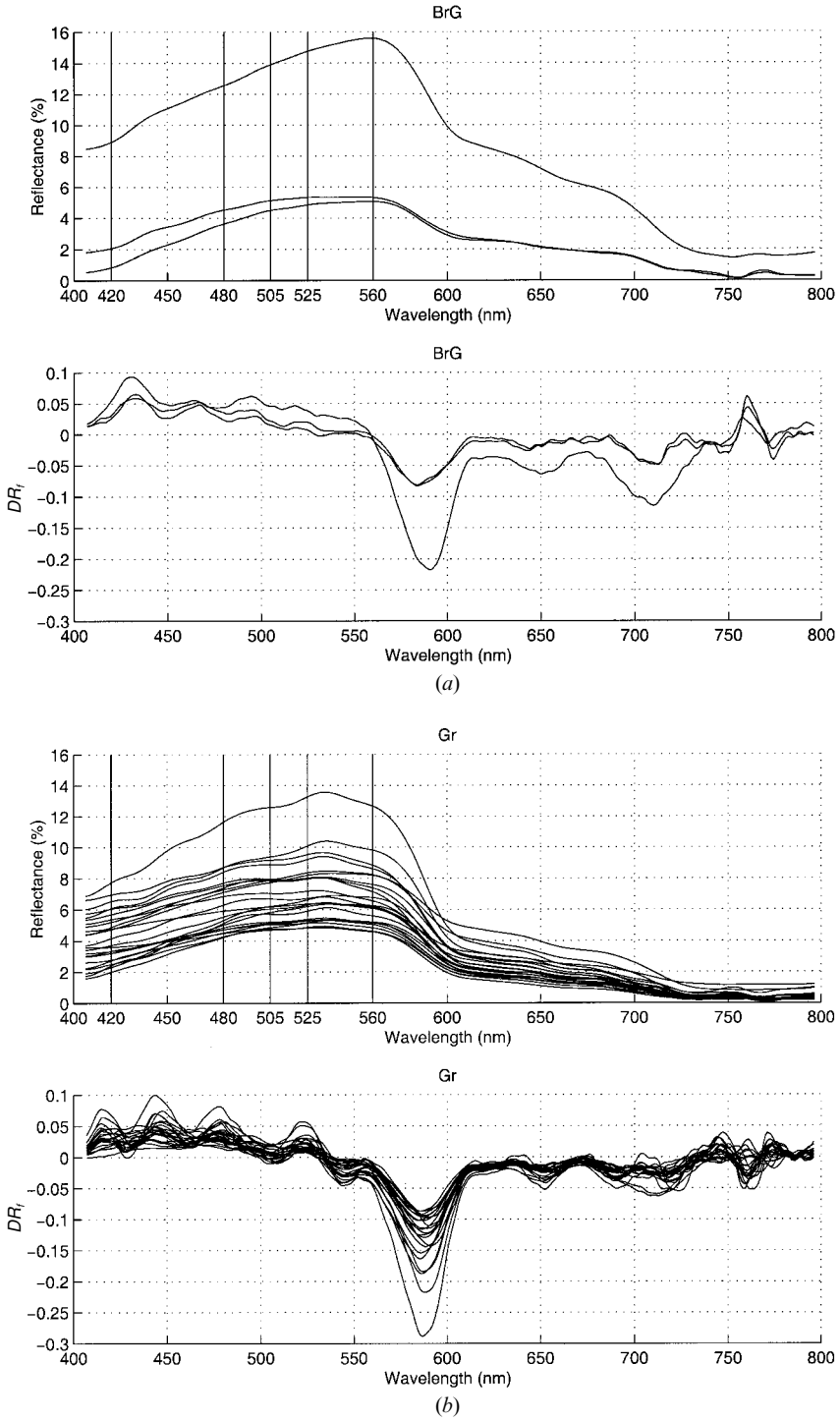

Figure 2. Reflectance spectra, measured in the Ebro river plume area, are presented at the top of the figure and first derivatives of the reflectance spectra, generated using mean-filter smoothing in conjunction with the finite approximation algorithm, are presented at the bottom. (*a*) BrG waters, (*b*) Gr waters, (*c*) BlG waters, (*d*) Bl waters.

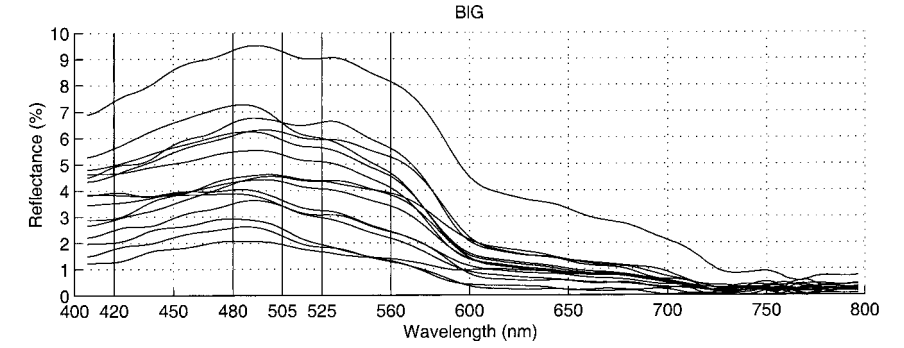
BIG
Reflectance (%)
Wavelength (nm)

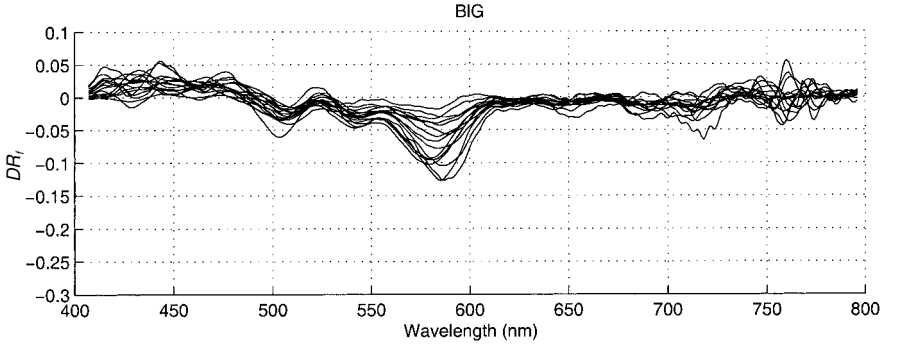
BIG
DR_f
Wavelength (nm)

(*c*)

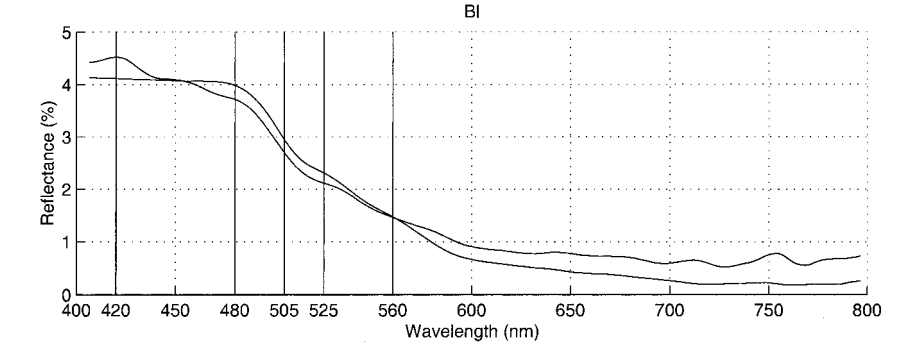
BI
Reflectance (%)
Wavelength (nm)

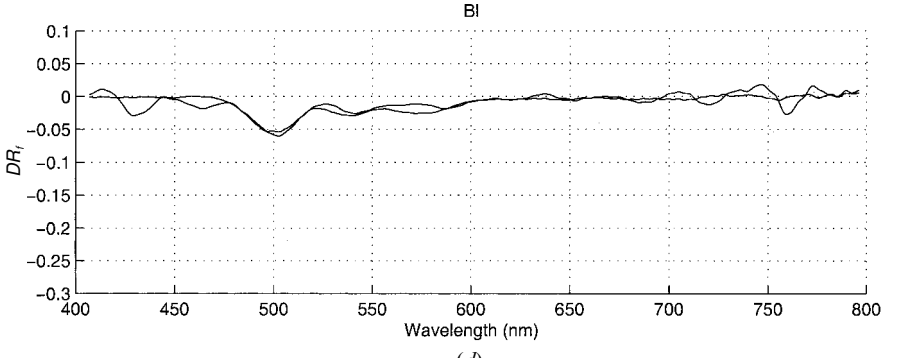
BI
DR_f
Wavelength (nm)

(*d*)

(Bricaud *et al.* 1981), and heterotrophic organisms (Morel and Ahn 1990, 1991) are characterized by high absorption coefficients in the blue region of the visible spectrum, where they have specific absorption coefficients close to those of phytoplankton (Agustí 1994), and by a sharp decrease of the absorption coefficient at longer wavelengths.

Four characteristic spectral shapes can be evidenced corresponding to four ranges of λ_{max}, namely >550 nm (brownish-green, hereafter noted BrG), 530–540 nm (green, Gr), 480–500 nm (blue-green, BlG) and 400–430 nm (blue, Bl). We have chosen a qualitative criterion of classification related to the dominant colour that could be perceived by a human eye. The reflectance spectra and the associated derivative spectra are shown on figure 2. Among the various methods developed for calculating derivatives (Tsai and Philpot 1998), a simple mean-filter algorithm was found to be convenient for smoothing our spectral data. The first derivatives were computed from discrete filtered $R(\lambda_i)$ values by:

$$\left.\frac{dR}{d\lambda}\right|_i \approx \frac{R(\lambda_j)-R(\lambda_i)}{\Delta\lambda} \tag{9}$$

where $\Delta\lambda$ is the band resolution, $\Delta\lambda=\lambda_j-\lambda_i$ and $\lambda_j>\lambda_i$. The derivative spectra generated are denoted DR_f in figure 2.

The derivative spectra exhibit, sometimes more than the reflectance spectra themselves, characteristic features which are very different from one class to another. The slopes of the reflectance spectra were computed within four significant spectral intervals: 420–480 nm, 480–505 nm, 505–525 nm and 525–560 nm (table 1). The slopes vary significantly both with water type and wavelength. It can be noted that $S_{480-505}$ is a good indicator to differentiate the water types. When $S_{480-505}$ values overlap, at the limit of two classes, the slopes are considered in a second spectral region to distinguish a water type. The reflectance spectra of figure 2 show that:

- Brownish-green water's spectra rapidly increase from 420 to 560 nm, present a marked peak at about 560 nm and then rapidly decrease. Moreover these spectra present a marked feature at 600 nm.
- Less turbid waters, green coloured, are characterized by a simultaneous decrease of reflectance amplitudes and slopes, from 400 to 700 nm. The feature at 600 nm is reduced. Examining the values of $S_{525-560}$ in addition to those of $S_{480-505}$ is an efficient tool to distinguish green waters and brownish-green waters.
- Evolution towards blue-green waters is accompanied by a decrease of reflectance amplitudes and slopes between 420 and 525 nm. The shift of the maximum towards shorter wavelengths is displayed by the shift of sign of

Table 1. Variations of the reflectance spectra slopes from 420 to 560 nm calculated for 42 reflectance spectra collected in the Ebro river mouth area.

Slopes (% μm^{-1})	$S_{420-480}$	$S_{480-505}$	$S_{505-525}$	$S_{525-560}$
BrG	41.6;59.9	24.0;52.6	7.0;44.2	−1.0;19.9
Gr	15.7;66.1	0.1;29.9	4.9;45.9	−32.2;−0.2
BlG	1.0;31.2	−41.8;2.7	−26.2;9.2	−41.5;−6.5
Bl	−14.5;−3.1	−50.4;−48.5	−22.2;−19.9	−23.9;−19.3

$S_{480-525}$ for most of the spectra. The feature at 600 nm still diminishes. $S_{505-525}$ brings fuller information to discriminate blue-green waters from green waters.

- Transition from blue-green to blue waters is obvious. $S_{420-480}$ becomes negative. $S_{480-505}$ and $S_{525-560}$ decrease up to the suppression of the peak at 480 nm. $S_{560-600}$ values decrease. These waters are blue coloured as $\lambda_{max} < 450$ nm but they were sampled in the coastal region. This explains the reflectance values of about 4% in the blue region. Blue and blue-green waters have distinct slope values in the spectral interval 420–480 nm.

The reflectance spectra shapes, representative of the four water types, are schematized in figure 3. Aming the various reflectance spectra measured, six have been chosen to characterize the reflectance variability in shape and amplitude between the water classes.

4.2. *Associated water quality parameters*

The reflectance model presented in §3 is inverted for the determination of $a_y(440)$ and m_r, using $R_{exp}(\lambda)$, *SPM* and *chl* measured during the field campaigns. Minimum, maximum and mean values of these parameters and of the Secchi disc depth, *SD*, are reported in table 2. As inherent optical properties were not measured during the field campaigns, absorption coefficient of yellow substance and sediment refractive index can only be compared with previously published data. $a_y(440)$ was found to vary from 0.02 to 0.45 m^{-1}. Reported values in the Mediterranean Sea for this parameter ranged from 0 to 0.03 m^{-1} in oceanic waters (Kirk 1994) and from 0.06

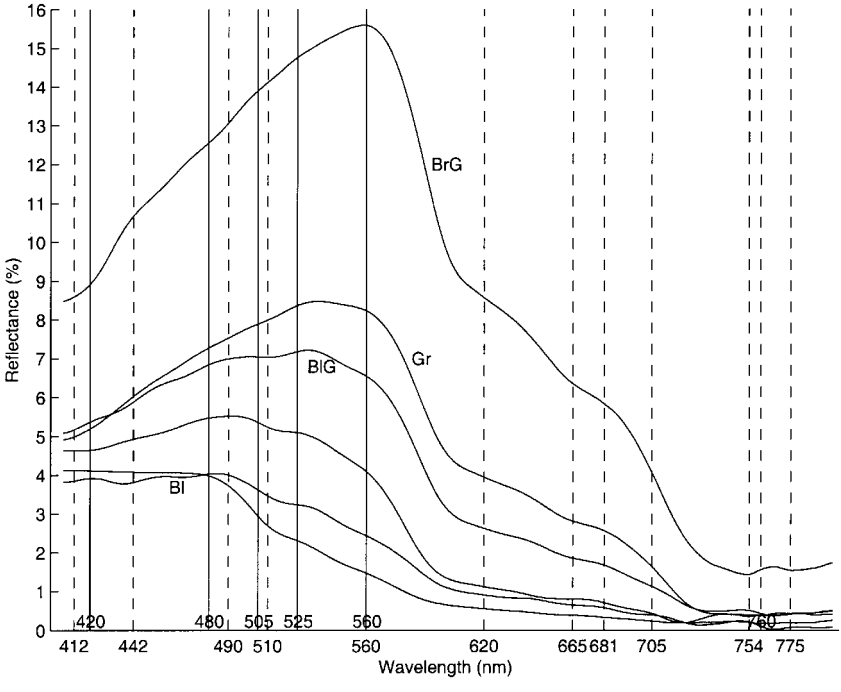

Figure 3. The optical classification and the associated typical shapes of the reflectance spectra. The characteristic slopes (full vertical bars) and MERIS sensor bands (dashed vertical bars) are also represented.

Table 2. Minimum, maximum and mean value (in italics) of suspended particulate matter concentration, *SPM*, chlorophyll a concentration, *chl*, absorption coefficient of yellow substance at 440 nm, $a_y(440)$, refractive index of sediment, m_r, and Secchi disc depth, *SD*. Number of samples per water mass class, *N*.

	N	*SPM* (mg l^{-1})	*chl* (μg l^{-1})	$a_y(440)$ (m^{-1})	m_r	*SD* (m)
BrG	3	1.82–14.37 *6.2*	0.94–1.79 *1.5*	0.23–0.45 *0.31*	1.13–1.18 *1.15*	3–6 *5*
Gr	22	1.14–7.07 *2.7*	0.57–2.09 *1.2*	0.07–0.25 *0.14*	1.11–1.20 *1.15*	3–6 *4.8*
BlG	15	0.31–6.27 *1.6*	0.22–1.40 *0.58*	0.03–0.13 *0.06*	1.10–1.14 *1.12*	5–17 *9.2*
Bl	2	0.52–1.12 *0.8*	0.17–0.27 *0.22*	0.02	1.09–1.11 *1.10*	17–28 *22.5*

to $0.65\,m^{-1}$ in coastal waters (Bricaud *et al.* 1981). m_r was found to vary from 1.09 to 1.20 which is close to the range 1.11–1.25 that can be found in literature for the common minerals (Aas 1996). Thus our estimates of $a_y(440)$ and m_r values are realistic.

The spatial variations of the water classes (figure 1) and of the water quality parameters are dependent on the position of the stations relative to the river mouth and to the plume front. Brownish-green, green and blue-green waters are generally located inside the plume. The more turbid waters, brownish-green coloured, are rather close to the Ebro river mouth. Their optical properties are mainly determined by mineral particles issued from erosion of the drainage basin and dissolved organic matter issued from terrestrial vegetation decay. *SPM* and $a_y(440)$ values decrease from brownish-green to blue waters and, at the same time, *SD* values increase. This originates from the dispersion of suspended particulate matter and yellow substance within the plume. The *SPM* decrease was enhanced by sedimentation of the largest particles brought by the river. Note that *SPM* and $a_y(440)$ values are small, even for the more turbid waters. This can be related to the low erosion and the scarcity of vegetation in the Ebro delta, assigned to rice-growing. Chlorophyll concentrations are on average greater than $1\,\mu g\,l^{-1}$ in brownish-green and green waters. These values are weak because of the non-bloom conditions during the two field campaigns performed in November and in July. Brownish-green and green waters are located close to the mouth. The higher values of chlorophyll concentrations in these waters in comparison with those in blue-green and blue waters may be explained as follows. The combination of relative transparency of the water ($SD \approx 5\,m$) and low river discharge favours the penetration of sun light and then biological activity in the presence of nutrients. When water masses move away from the mouth to reach oceanic waters, we can assume that nutrients become more and more scarce. The lack of nutrients induces a slow down of phytoplankton production in blue-green waters and finally leads to blue waters, poor in dissolved and particulate matter.

4.3. *Retrieval of water quality parameters from first derivative reflectance*

The method is based on the determination of empirical relationships between first-order derivative reflectance spectra and *SPM*, *chl*, $a_y(440)$ and m_r, respectively. The study concerns Gr and BlG waters which were more widely sampled than BrG and Bl waters. Table 3 reports the different relationships obtained. For each colour and for each water quality parameter X, the wavelength considered is the wavelength corresponding to the highest correlation coefficient between DR_f and X. The reliability of the proposed relationships is estimated by calculating the correlation coefficient, r, and the associated confidence level, $(1-\alpha)$. To test whether there is a significant linear correlation, we consider that when the theoretical correlation coefficient, ρ, is equal to 0, the statistic test $t = r\sqrt{N-2}/\sqrt{1-r^2}$ has a Student's t distribution with $N-2$ degrees of freedom (Spiegel 1988). N is the number of samples per water mass class.

The results of table 3 indicate that *SPM* is correlated with wavelengths in the red part of the visible spectrum: 708 nm (BrG), 786 nm (Gr), 625 nm (BlG). This is in agreement with the results of previous studies on derivative reflectance spectroscopy (table 4). Correlations were obtained between *SPM* and $DR(727)$ (Chen *et al.* 1992); turbidity and $DR(720)$ (Goodin *et al.* 1993); and turbidity and $DR(628)$ (Fraser 1998). Experimental *chl* values were correlated with wavelengths in the red for BrG waters (771 nm), in the green for Gr waters (552 nm) and in the blue (485 nm)

Table 3. Correlation models between first derivative reflectance features and water quality parameters. Number of samples per water mass class, N, slope, a, intercept, b, correlation coefficient, r and confidence level, $(1-\alpha)$.

Colour	Concentration	Algorithm	N	a	b	r	$(1-\alpha)$ (%)
BrG	1.8–14.4 mg l^{-1}	$SPM = a\ DR_f(708) + b$	3	−185	−6.50	0.999	97.5
	0.9–1.8 μg l^{-1}	$chl = a\ DR_f(771) + b$	3	−108	-2.82×10^{-2}	0.998	97.5
		$a_y(440) = a\ DR_f(561) + b$	3	24.6	0.588	0.999	97.5
		$m_r = a\ DR_f(562) + b$	3	3.75	1.21	0.999	97.5
Gr	1.1–10.5 mg l^{-1}	$SPM = a\ DR_f(786) + b$	22	455	3.53	0.607	99.5
	0.6–3.4 μg l^{-1}	$chl = a\ DR_f(552) + b$	22	34.7	1.91	0.579	99.5
		$a_y(440) = a\ DR_f(535) + b$	22	5.81	0.155	0.868	99.5
		$m_r = a\ DR_f(489) + b$	22	1.88	1.10	0.619	99.5
BlG	0.3–6.3 mg l^{-1}	$SPM = a\ DR_f(625) + b$	15	−296	0.733	0.898	99.5
	0.2–1.4 μg l^{-1}	$chl = a\ DR_f(485) + b$	15	25.8	0.410	0.779	99.5
		$a_y(440) = a\ DR_f(707) + b$	15	−1.32	4.49×10^{-2}	0.609	99
		$m_r = DR_f(745) + b$	15	0.490	1.12	0.450	95

Table 4. Correlation models between first derivative reflectance features and water quality parameters. Slope, a, intercept, b, and correlation coefficient, r.

	Concentration	Model form	r
Chen *et al.* (1992)	0–590 mg l^{-1}	$SPM = a\ DR(560) + b$	0.97
	27–103 mg l^{-1}	$SPM = a\ DR(727) + b$	0.99
		$SPM = a\ (DR(727) - DR(560)) + b$	0.99
Goodin *et al.* (1993)	2.8–3.3 NTU	$turb = a\ DR(720) + b$	0.95
Rundquist *et al.* (1996)	340–2190 μg l^{-1}	$chl = a\ DR(690) + b$	0.99
	156–277 μg l^{-1}	$chl = a\ DR(483) + b$	0.98
Han and Rundquist (1997)	71–590 μg l^{-1}	$chl = a\ DR(690) + b$	0.82
Fraser (1998)	1–82 NTU	$turb = a\ DR(429) + b$	0.80
		$turb = a\ DR(628) + b$	0.77
		$turb = a\ (DR(429) \times DR(628)) + b$	0.81
		$turb = a\ DR(429) + b\ DR(628) + c\ DR(695) + d$	0.83
	1–171 μg l^{-1}	$chl = a\ DR(695) + b$	0.63
		$chl = a\ (DR(429) \times DR(695)) + b$	0.67
		$chl =$ $a\ DR(429) + b\ DR(695) + c(DR(429) \times DR(695)) + d$	0.71

NTU, nephelometric turbidity units; turb, turbidity.

for BlG waters. From table 4, published data indicate that *chl* can be correlated with $DR(483)$ (Rundquist *et al.* 1996), $DR(690)$ (Han and Rundquist 1997) and $DR(695)$ (Fraser 1998). The range of concentrations studied by Fraser (1998) closely corresponds to that of brownish-green waters and this author also found the wavelengths of highest correlation in the red. Our correlation coefficients are lower than those of table 4. This probably originates from the low values of *SPM* and *chl* and from the narrow ranges of variation of these parameters. Nevertheless the confidence level is between 95 and 99.5% which indicates that the correlation relationships are quite reliable. $a_y(440)$ can be deduced from the first derivative of reflectance in the green (BrG: 561 nm, Gr: 535 nm, BlG: 496 nm). m_r is weakly correlated with the first derivative ($r = 0.62$ for Gr waters and $r = 0.45$ for BlG waters). The most interesting correlations were found between $a_y(440)$ and $DR_f(535)$ for Gr waters ($r = 0.85$) and between *SPM* and $DR_f(625)$ for BlG waters ($r = 0.90$).

The scatter plots of *chl* and *SPM* for Gr and BlG waters, using the empirical models of table 3, are given in figure 4 and figure 5, respectively. Horizontal bars indicate the experimental uncertainties on SPM_{exp} and chl_{exp} values (see §2). The root mean-square errors on the determination of *SPM*, rms(*SPM*), and *chl*, rms(*chl*), are plotted with dashed lines at $X_{corr} \pm \text{rms}(X)/2$. rms($X$) values are reported in table 5 as well as those of the corresponding coefficient of variation, $V(X)$. The values of $V(X)$ allows us to compare the standard errors on the determination of X as the ranges of concentrations considered are different in Gr and BlG waters.

In figure 4, the estimates of *chl* appear evenly distributed around the regression lines, whatever the order of magnitude of chl_{exp}. Forty-five per cent of the estimates are set between the dashed lines for Gr waters and 53% for BlG waters. The

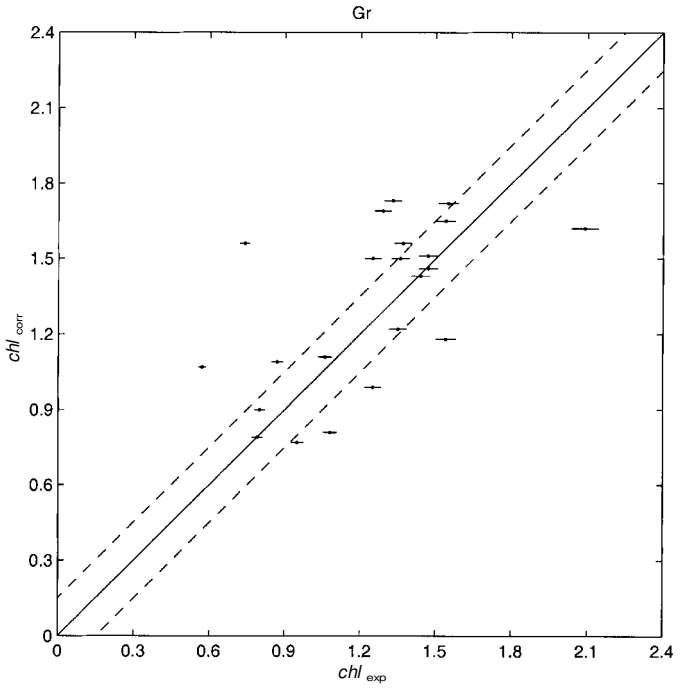

(*a*)

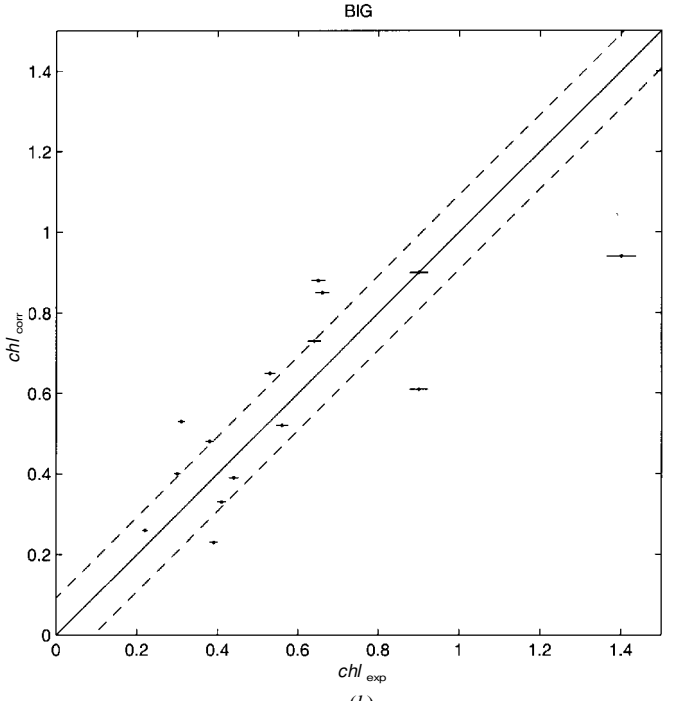

(*b*)

Figure 4. The relationship between measured chlorophyll concentration, chl_{exp} and estimated chlorophyll concentration using empirical models, chl_{corr}. (*a*) Gr waters, (*b*) BIG waters. 1:1, solid line; 1:1 $\pm$ rms(chl)/2, dashed line; $chl_{exp} \pm \Delta chl_{exp}$, bar.

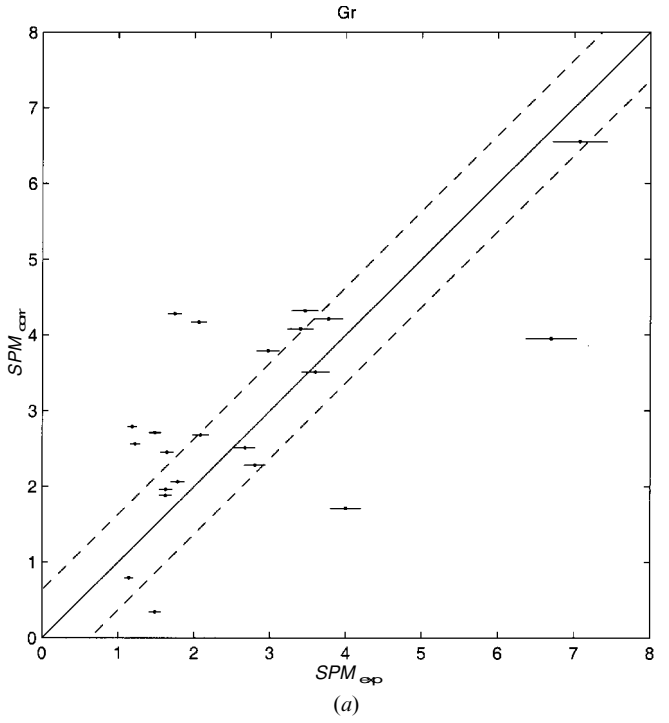

(*a*)

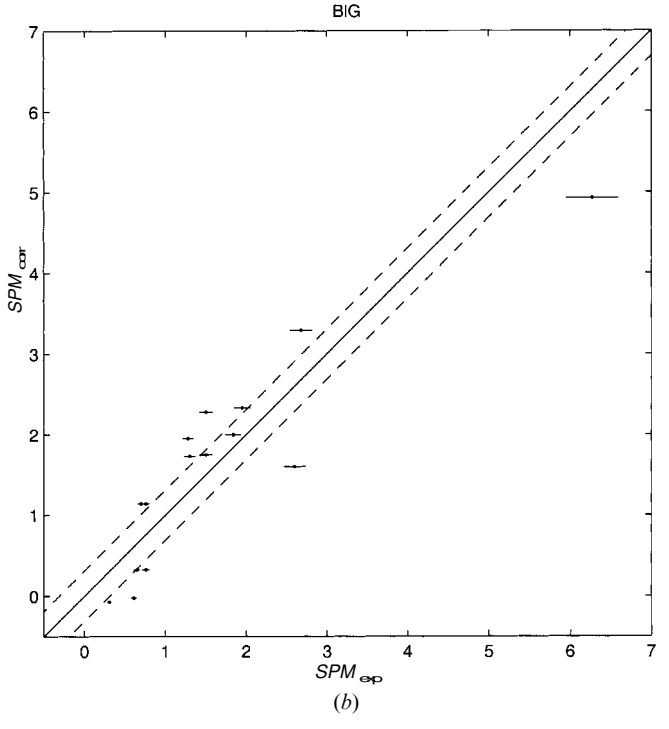

(*b*)

Figure 5. The relationship between measured SPM concentration, SPM_{exp}, and estimated SPM concentration using empirical models, SPM_{corr}. (*a*) Gr waters, (*b*) BlG waters. 1:1, solid line; $1{:}1 \pm \text{rms}(SPM)/2$, dashed line; $SPM_{exp} \pm \Delta SPM_{exp}$, bar.

Table 5. Determination of water quality parameters from empirical models (correlations), from inversion of the reflectance model (simulation 1) and by merging the two methods (simulation 3). Suspended particulate matter concentration, *SPM*, chlorophyll a concentration, *chl*. Root mean-square errors on *SPM* estimates, rms(*SPM*), and *chl* estimates, rms(*chl*) and associated coefficients of variation, *V*(*SPM*) and *V*(*chl*).

	Gr				BlG			
	rms (*SPM*) ($mg\,l^{-1}$)	*V* (*SPM*) (%)	rms (*chl*) ($\mu g\,l^{-1}$)	*V* (*chl*) (%)	rms (*SPM*) ($mg\,l^{-1}$)	*V* (*SPM*) (%)	rms (*chl*) ($\mu g\,l^{-1}$)	*V* (*chl*) (%)
Correlations	1.26	47	0.30	25	0.62	39	0.18	31
Simulation 1	1.09	40	2.58	215	0.48	30	0.82	141
Simulation 2	1.03	38	2.35	196	0.45	28	2.03	350
Simulation 3	1.19	44	0.30	25	0.56	35	0.18	31

correlation relationship for the determination of *chl* is somewhat more precise for Gr waters ($V(chl)=25\%$) than for BlG waters ($V(chl)=31\%$). Examination of the scatter plots of *SPM* (figure 5) shows that 50% of the estimates are set between the dashed lines on figure 5(*a*) whereas only 27% fill this condition on figure 5(*b*) but the points are less dispersed from the 1:1 line. The empirical models give better results when applied to BlG waters as $V(SPM)$ is equal to 39% ($V(SPM)=47\%$ for Gr waters). On the one hand, the empirical models appear more accurate for the determination of *chl* ($V(chl)<31\%$) than for the determination of *SPM* ($V(SPM)>39\%$). On the other hand, *chl* is more precisely retrieved in Gr waters ($V(chl)=25\%$) and *SPM* is more precisely retrieved in BlG waters ($V(SPM)=39\%$).

The method presented here to estimate water quality parameters is empirical. A second approach, based on the inversion of a reflectance model and on the colour classification, is proposed to improve the results.

5. Retrieval of water quality parameters using the reflectance model and the colour classification

The inversion of the reflectance model presented in §3 using our colour classification can be envisaged in three ways:

1. Determination of chl_{mod}, SPM_{mod} and $a_y(440)_{mod}$ from m_r (simulation 1)
2. Determination of chl_{mod} and SPM_{mod} from m_r and $a_y(440)$ (simulation 2)
3. Determination of chl_{mod}, SPM_{mod} and m_{rmod} from $a_y(440)$.

The third possibility is eliminated as both m_r and *SPM* cannot be determined when using Mie theory for b_{bs} (Forget *et al.* 1999). Concerning simulations 1 and 2, m_r and/or $a_y(440)$ values are the mean values characterizing the water mass classes as deduced from table 2: (1.15, $0.14\,m^{-1}$) for Gr waters and (1.12, $0.06\,m^{-1}$) for BlG waters. The simulations results are reported in table 5.

SPM estimates are improved compared with the results obtained using the empirical method. For Gr waters, rms(*SPM*) is reduced by 13% (simulation 1) and by 18% (simulation 2). The decrease of rms(*SPM*) is slightly more pronounced for BlG waters: 23% (simulation 1) and 27% (simulation 2). On the scatter plot of *SPM* estimates for Gr waters (figure 6(*a*)) 60% of the points are set between the dashed lines but the semi-analytical method fails to estimate concentrations greater than $3\,mg\,l^{-1}$. For BlG waters, 60% of the points are set between the dashed lines

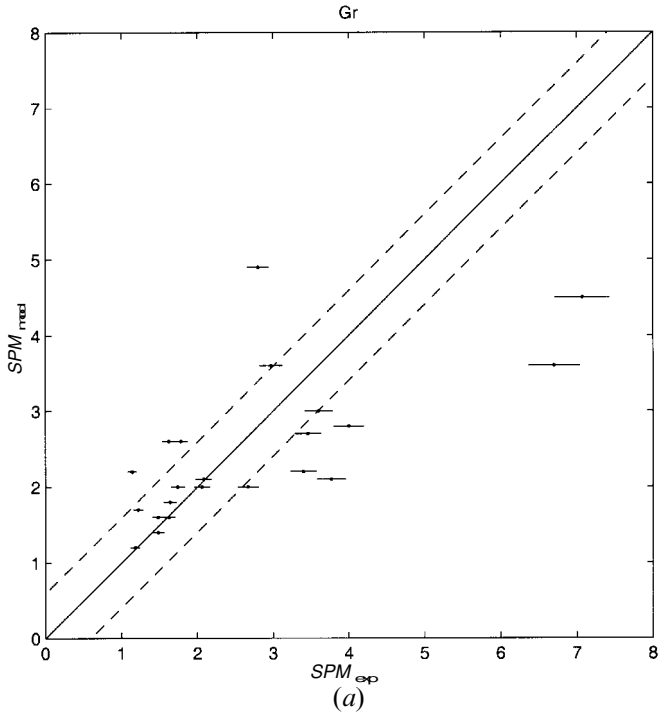

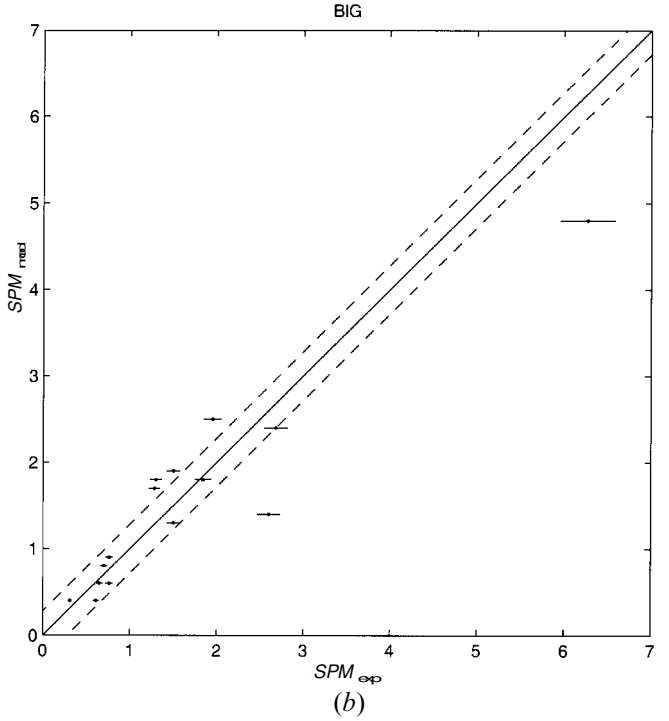

Figure 6. The relationship between measured SPM concentration, SPM_{exp}, and estimated SPM concentration using inversion of a reflectance model, SPM_{mod}. (*a*) Gr waters, (*b*) BIG waters. 1:1, solid line; $1{:}1 \pm \text{rms}(SPM)/2$, dashed line; $SPM_{exp} \pm \Delta SPM_{exp}$, bar.

(figure 6(*b*)). In that case, the dispersion of the points is significantly reduced, in particular for *SPM* values less than $1\,mg\,l^{-1}$.

chl is less precisely retrieved ($V(chl) > 100\%$) than when using the empirical models ($V(chl) = 31\%$). For Gr waters, rms(*chl*) is multiplied by 8.6 (simulation 1) and 7.8 (simulation 2). In the case of BlG waters, the multiplicative factors are equal to 4.6 (simulation 1) and 11 (simulation 2). The less accurate determination of *chl* originates from two main causes. Hoge and Lyon (1996) showed that IOP retrieval errors using a linear inversion method are strongly dependent on the phytoplankton model used in equations (5) and (7). The error in the retrieval of *chl* is enhanced because of the uncertainties concerning the modelling of the phytoplankton optical properties in coastal waters. Moreover the time periods of the field campaigns, during non-bloom conditions, are such that absorption by phytoplankton and related products is low. Absorption by yellow substance is dominant and induces a low sensitivity of reflectance spectra to the phytoplanktonic component.

Individual $a_y(440)$ values deduced from SPM_{exp} and chl_{exp} values ($a_y(440)$, §4.2) and from simulation 1 ($a_y(440)_{mod}$) are plotted on figure 7. The slope of the regression line is close to 1 and the rms difference between $a_y(440)$ and $a_y(440)_{mod}$ is $0.03\,m^{-1}$. Furthermore rms(*SPM*) and rms(*chl*) are very close in both cases. We conclude that simulation 1 should be preferred to simulation 2 which uses mean values of $a_y(440)$.

We investigated the improvement on *SPM* estimates brought by merging the empirical and the semi-analytical methods. SPM_{mod} and $a_y(440)_{mod}$ are now obtained from m_r and chl_{corr} (simulation 3). The results of table 5 show that rms(*SPM*) and $V(SPM)$ values are a little greater than those obtained from simulation 1.

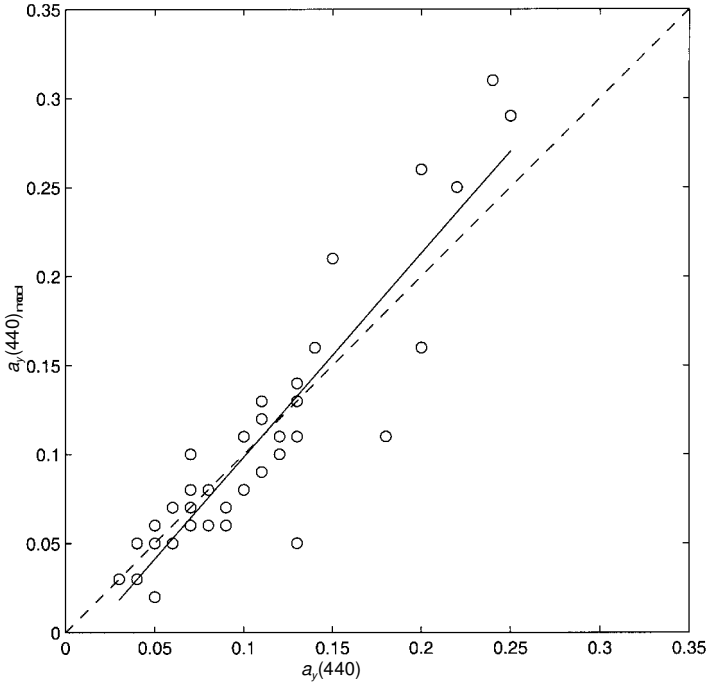

Figure 7. The relationship between $a_y(400)$ values deduced from the colour classification, $a_y(440)$, and $a_y(440)$ values estimated using inversion of a three component reflectance model, $a_y(440)_{mod}$. 1:1, dashed line; regression, solid line.

6. Discussion

The determination of chlorophyll a concentration is much more accurate using the correlation method presented in §4.3 ($V(chl)=25\%$ (Gr) and 31% (BlG)). Nevertheless, suspended particulate matter concentration is estimated with a similar precision by applying the empirical method (correlations: $V(SPM)=47\%$ (Gr) and 39% (BlG)) or the semi-analytical method (simulation 1: $V(SPM)=40\%$ (Gr) and 30% (BlG)). The application of an empirical method implies the disposal of a lot of experimental data, always affected with errors. The semi-analytical method can be used all the time but the calculations are more time-consuming. Consequently *SPM* computation will be conditioned by the nature and the quantity of experimental data collected in the studied area.

The study was realized from experimental data collected during two time periods: November 96 (Fliper1) and July 97 (Fliper3). We can consider whether the results obtained in §5.2 are improved by treating the two types of data separately. The colour classifications obtained for the two sets of data are given in table 6. Fliper1 BrG waters are characterized by a low particulate load ($SPM<2.5\,\mathrm{mg\,l^{-1}}$, $chl<2\,\mu\mathrm{g\,l^{-1}}$) and the highest dissolved organic matter concentrations $a_y(440)>0.25\,\mathrm{m^{-1}}$). Fliper3 BrG water is characterized by the highest SPM concentration ($SPM=14.4\,\mathrm{mg\,l^{-1}}$), but chlorophyll and yellow substance are in quantities similar to those found in Fliper1 waters. Examination of the Gr water colour classification shows that:

1. SPM concentrations were twofold greater during Fliper3;
2. *chl* mean values were identical during the two time periods but the range of *chl* values was wider during Fliper1;
3. the range of $a_y(440)$ values was the same during the two time periods but the mean value was higher during Fliper1.

Fliper3 Gr waters are thus characterized by significantly greater suspended sediment concentrations whereas *chl* and $a_y(440)$ values are similar for the two experiments. The colour classification of BlG waters shows that:

1. SPM concentrations were twofold greater during Fliper3;
2. the water mass was richer in chlorophyll during Fliper1;
3. there was a little bit more yellow substance during Fliper1.

Fliper1 BlG waters are chlorophyll and yellow substance dominated whereas Fliper3 BlG waters are sediment dominated. Bl waters were sampled only during Fliper3.

Empirical relationships relating X and DR_f were calculated for the two water types. The wavelengths of highest correlation coefficient, λ_{corr}, are given in table 7. Whatever the water quality parameter considered, λ_{corr} values are different for the two sampling periods. These differences originate from the distinct characteristics of the water mass considered which was previously evidenced by examining the two colour classifications and from the low number of water samples.

The method presented in §5 was applied separately to the two datasets (table 8). If we compare the results of table 5 and table 8, we can see that *SPM* estimates are improved for Fliper1 waters but not for Fliper3 waters except when correlation relationships are applied to BlG waters. Concerning *chl*, no improvement was observed. The errors in the retrieval of *SPM* and *chl* are not significantly reduced and the size of the dataset available to realize each statistical study is lowered. Consequently we can conclude that it is more convenient to establish a colour

Table 6. Minimum, maximum and mean value (in italics) of suspended particulate matter concentration, *SPM*, chlorophyll a concentration, *chl*, absorption coefficient of yellow substance at 440 nm, $a_y(440)$, refractive index of sediment, m_r and Secchi disc depth, *SD*. Number of samples per water mass class, *N*. Time period of the measurements: November 96 (Fliper1) and July 97 (Fliper3).

		N	*SPM* (mg l^{-1})	*chl* (μg l^{-1})	$a_y(440)$ (m^{-1})	m_r	*SD* (m)
BrG	Fliper1	2	1.82–2.38 *2.1*	0.94–1.78 *1.36*	0.26–0.45 *0.35*	1.15–1.18 *1.16*	6
	Fliper3	1	14.37	1.79	0.23	1.13	3
Gr	Fliper1	13	1.14–4.00 *1.77*	0.87–1.55 *1.35*	0.08–0.25 *0.15*	1.13–1.20 *1.16*	3.5–6 *5.1*
	Fliper3	9	2.67–7.07 *4.70*	0.57–2.09 *1.31*	0.07–0.20 *0.11*	1.08–1.19 *1.13*	2.5–5.5 *4.1*
BlG	Fliper1	8	0.31–2.68 *1.16*	0.22–1.40 *0.63*	0.05–0.13 *0.07*	1.10–1.14 *1.12*	5–17 *10*
	Fliper3	7	0.70–6.27 *2.20*	0.31–0.90 *0.52*	0.03–0.09 *0.05*	1.10–1.14 *1.12*	5.5–11 *8.2*
Bl	Fliper3	2	0.52–1.12 *0.8*	0.17–0.27 *0.22*	0.02	1.09–1.11 *1.10*	17–28 *22.5*

Table 7. Wavelength of highest correlation coefficient between DR_f and the water quality parameters, λ_{corr} (nm).

		SPM	*chl*	$a_y(440)$	m_r
Gr	All	786	552	535	489
	Fliper1	679	635	535	533
	Fliper3	560	786	704	681
BlG	All	625	485	707	745
	Fliper1	624	475	537	728
	Fliper3	711	713	673	782

Table 8. Determination of water quality parameters from empirical models (correlations) and from inversion of the reflectance model (simulation 1). Suspended particulate matter concentration, *SPM*, chlorphyll a concentration, *chl*. Root mean-square errors on *SPM* estimates, rms(*SPM*), and *chl* estimates, rms(*chl*).

		Fliper1		Fliper3	
		rms(*SPM*) ($mg\,l^{-1}$)	rms(*chl*) ($\mu g\,l^{-1}$)	rms(*SPM*) ($mg\,l^{-1}$)	rms(*chl*) ($\mu g\,l^{-1}$)
Gr	Correlations	0.47	0.10	1.34	0.49
	Simulation 1	0.58	0.98	1.70	4.36
BlG	Correlations	0.17	0.20	0.35	0.06
	Simulation 1	0.26	0.83	0.65	0.82

classification on a larger set of data instead of making an area and season specific classification.

7. Conclusion

Analysis of the shapes of reflectance spectra measured in the Ebro river plume allows us to classify differently coloured water types, the water colour referring here to the wavelength of the reflectance spectra peak. An empirical method and a semi-analytical method have been presented to estimate four water quality parameters namely chlorophyll concentration, suspended sediment concentration, sediment refractive index and absorption coefficient of yellow substance at 440 nm.

Associating the two methods allows the concurrent estimate of suspended particulate matter and chlorophyll a concentrations in coastal waters of low turbidity. *chl* and *SPM* values are recovered with relatively low rms errors: $\text{rms}(chl) = 0.30\,\mu g\,l^{-1}$ and $\text{rms}(SPM) = 1.09\,mg\,l^{-1}$ in green waters, $\text{rms}(chl) = 0.18\,\mu g\,l^{-1}$ and $\text{rms}(SPM) = 0.48\,mg\,l^{-1}$ in blue-green waters. The procedure to compute *chl*, *SPM* along with $a_y(440)$ consists of evaluating *chl* from correlation algorithms and *SPM* and $a_y(440)$ from a reflectance model in which inputs are the mean m_r value characteristic of the water class. The parameter m_r cannot be measured directly and is very sensitive to the water composition and to a lesser extent, to pressure, temperature and salinity (Kirk 1994). We used an extensive dataset of *chl* and *SPM* to determine the mean m_r values corresponding to each water class. Moreover we found that using mean $a_y(440)$ values as inputs in the reflectance model did not significantly improve the accuracy of *SPM* and *chl* estimates.

The colour classification also finds applications in satellite remote sensing. Let

us consider the example of the MERIS instrument, equipped with 15 spectral bands in the visible and in the near-infrared regions. The central wavelengths of these bands are shown on figure 3 (dotted vertical bars) as well as the characteristic slopes of the reflectance spectra (full vertical bars). Band 3 (485–495 nm) and band 4 (505–515 nm) are suitable to determine $S_{480-505}$ and then to distinguish the water classes. In Gr waters band 12 (767.5–782.5 nm) and band 5 (555–565 nm) could be used to estimate SPM concentration ($\lambda_{corr} = 786$ nm) and chlorophyll concentration ($\lambda_{corr} = 552$ nm), respectively. In BlG waters band 6 (615–625 nm) and band 3 (485–495 nm) could be used to estimate SPM concentration ($\lambda_{corr} = 625$ nm) and chlorophyll concentration ($\lambda_{corr} = 485$ nm), respectively.

This study demonstrates the suitability of associating optical measurements and water colour classification to provide reliable estimates of water quality parameters. However it should be noted that in the present study the same dataset of optical and water quality quantities has been used to provide the statistics about the different water classes and to assess the proposed inversion procedure. It is necessary now to verify that our statistical characterization of water types, in terms of empirical relationships between derivative reflectance and *chl* and of characteristic m_r values, can be routinely used over the Ebro delta site. This could be done on the occasion of future field campaigns.

Acknowledgments

This study was supported by the European Community MAST3 Program (FANS, contract MAS3-CT95-0037). The authors are grateful to all members of LSEET, especially J. Gaggelli and G. Rougier, of Laboratoire Arago and of CEAB who participated in the field campaign and the data analysis. Special thanks to J. J. Naudin and L. Auriol who measured the SPM concentrations and to A. Cruzado and Z. Velasquez who measured the chlorophyll concentrations.

References

Aas, E., 1996, Refractive index of phytoplankton derived from its metabolite composition. *Journal of Plankton Research*, **18**, 2223–2249.

Agustí, S., 1994, Planktonic size structure and the photon budget of the euphotic ocean. In *The Size Structure and Metabolism of the Pelagic Ecosystem*, edited by J. Rodríguez and W. K. W. Li (Barcelona: Institut de Sciencès del Mar), pp. 109–117.

Ahn, Y. H., Bricaud, A., and Morel, A., 1992, Light backscattering efficiency and related properties of some phytoplankters. *Deep-Sea Research*, **39**, 1835–1855.

André, J. M., and Morel, A., 1991, Atmospheric corrections and interpretation of marine radiances in CZCS imagery. *Oceanologica Acta*, **14**, 3–22.

Antoine, D., Morel, A., and André, J. M., 1995, Algal pigment distribution and primary production in the Eastern Mediterranean as derived from Coastal Zone Scanner observations. *Journal of Geophysical Research*, **100**, 16 193–16 209.

Baker, K. S., and Smith, R. C., 1979, Quasi-inherent characteristics of the diffuse attenuation coefficient for irradiance. *Proceedings Ocean Optics VI*, SPIE, **208**, pp. 60–63.

Blough, N. V., Zafiriou, O. C., and Bonilla, J., 1993, Optical absorption spectra of waters from the Orinoco River outflow: Terrestrial input of colored organic matter to the Caribbean. *Journal of Geophysical Research*, **98**, 2271–2278.

Bricaud, A., Morel, A., and Prieur, L., 1981, Absorption by dissolved organic matter of the sea (yellow substance) in the UV and visible domains. *Limnology and Oceanography*, **26**, 43–53.

Bricaud, A., Babin, M., Morel, A., and Claustre, H., 1995, Variability in the chlorophyll-specific absorption coefficients of natural phytoplankton: Analysis and parameterization. *Journal of Geophysical Research*, **100**, 13 321–13 332.

Carder, K. L., Hawes, S. K., Baker, K. A., Smith, R. C., Steward, R. G., and Mitchell,

B. G., 1991, Reflectance model for quantifying chlorophyll a in the presence of productivity degradation products. *Journal of Geophysical Research*, **96**, 20 599–20 611.

Chen, Z., Curran, P. J., and Hansom, J. D., 1992, Derivative reflectance spectroscopy to estimate suspended sediment concentration. *Remote Sensing of Environment*, **40**, 67–77.

Duarte, C. M., Agustí, S., Satta, M. P., and Vaqué, D., 1998, Partitioning particulate light absorption: A budget for a Mediterranean bay. *Limnology and Oceanography*, **43**, 236–244.

Durand, N., Fiandrino, A., Fraunié, P., Ouillon, S., Forget, P., and Naudin, J. J., 2000, Suspended matter dispersion in the Ebro ROFI: An integrated approach. *Continental Shelf Research* (in revision).

Fisher, J., Doerffer, R., and Grassl, H., 1986, Factor analysis of multispectral radiances over coastal and open ocean water based on radiative transfer calculations. *Applied Optics*, **25**, 448–456.

Forget, P., and Ouillon, S., 1998, Surface suspended matter off the Rhône river mouth from visible satellite imagery. *Oceanologica Acta*, **21**, 739–749.

Forget, P., Ouillon, S., Lahet, F., and Broche, P., 1999, Inversion of reflectance spectra of non-chlorophyllous turbid coastal waters. *Remote Sensing of Environment*, **68**, 264–272.

Fraser, R. N., 1998, Hyperspectral remote sensing of turbidity and chlorophyll a among Nebraska Sand Hills lakes. *International Journal of Remote Sensing*, **19**, 1579–1589.

Goodin, D. G., Han, L., Fraser, R. N., Rundquist, D. C., and Stebbins, W. A., 1993, Analysis of suspended solids in water using remotely sensed high resolution derivative spectra. *Photogrammetric Engineering and Remote Sensing*, **59**, 505–510.

Gordon, H. R., Brown, O. B., and Jacobs, M. M., 1975, Computed relations between the inherent and apparent optical properties of a flat homogeneous ocean. *Applied Optics*, **14**, 417–427.

Gower, J. F. R., Lin, S., and Borstad, G. A., 1984, The information content of different optical spectral ranges for remote chlorophyll estimation in coastal waters. *International Journal of Remote Sensing*, **5**, 239–364.

Guillèn, J., and Palanques, A., 1992, Sediment dynamics and hydrodynamics in the lower course of a river highly regulated by dams: the Ebro river. *Sedimentology*, **39**, 567–579.

Han, L., and Rundquist, D. C., 1997, Comparison of NIR/red ratio and first derivative of reflectance in estimating algal-chlorophyll concentration: A case study in a turbid reservoir. *Remote Sensing of Environment*, **62**, 253–261.

Hoge, F. E., and Lyon, P. E., 1996, Satellite retrieval of inherent optical properties by linear matrix inversion of oceanic radiance models: An analysis of model and radiance measurements errors. *Journal of Geophysical Research*, **101**, 16 631–16 648.

Ibañez, C., Pont, D., and Prat, N., 1997, Characterization of the Ebre and Rhône estuaries: A basis for defining and classifying salt-wedge estuaries. *Limnology and Oceanography*, **42**, 89–101.

Jerlov, N. G., 1951, Optical studies of ocean water. *Report Swedish Deep-Sea Expedition*, **3**, 1–59.

Jerlov, N. G., 1976, *Marine Optics* (Amsterdam: Elsevier).

Kirk, J. T. O., 1994, *Light and Photosynthesis in Aquatic Ecosystems*, 2nd edn (Cambridge: Cambridge University Press).

Lahet, F., Ouillon, S., and Forget, P., 2000, A three component model of ocean colour and its application in the Ebro river mouth area. *Remote Sensing of Environment*, **72**, 181–190.

Morel, A., 1988, Optical mdoelling of the upper ocean in relation to its biogenous matter content (case 1 waters). *Journal of Geophysical Research*, **93**, 10 749–10 768.

Morel, A., and Gordon, H. R., 1980, Report of the working group on ocean colour. *Boundary Layer Meteorology*, **18**, 343–355.

Morel A., and Ahn, Y. H., 1990, Optical efficiency factors of free-living bacteria: Influence of bacterioplankton upon the optical properties and particulate organic carbon in oceanic waters. *Journal of Marine Research*, **48**, 145–175.

Morel, A., and Ahn, Y. H., 1991, Optics of heterotrophic nanoflagellates and ciliates: A tentative assessment of their scattering role in oceanic waters compared to those of bacterial and algal cells. *Journal of Marine Research*, **49**, 177–202.

MOREL, A., and PRIEUR, L., 1977, Analysis of variations in ocean color. *Limnology and Oceanography*, **22**, 709–722.

MURA, M. P., AGUSTÍ, S., CEBRÍAN, J., and SATTA, M. P., 1996, Seasonal variability of phytoplankton biomass and composition in Blanes Bay (1992–1994). In *Seasonality in Blanes Bay: A Paradigm of the Northwest Mediterranean Littoral.* Publicaciones Especiales IEO no 22 (Madrid: Instituto Español de Oceanografía), pp. 23–29.

NAUDIN, J. J., CAUWET, G., CHRETIENNOT-DINET, M. J., DENIAUX, B., DEVENON, J. L., and PAUC, H., 1997, River discharge and wind influence upon particulate transfer at the land-sea interaction. Case study of the Rhône river plume. *Estuarine, Coastal and Shelf Science*, **45**, 303–316.

PALANQUES, A., and DRAKE, D. E., 1990, Distribution and dispersal of suspended particulate matter on the Ebro continental shelf, northwestern Mediterranean Sea. *Marine Geology*, **95**, 193–206.

PALANQUES, A., PLANA, F., and MALDONADO, A., 1990, Recent influence of man on the Ebro margin sedimentation system, northwestern Mediterranean Sea. *Marine Geology*, **95**, 247–263.

PELEVIN, V. N., and RUTKOVSKAYA, V. A., 1977, On the optical classification of ocean waters from the spectral attenuation of solar radiation. *Oceanology*, **17**, 28–32.

POPE, R. M., and FRY, E. S., 1997, Absorption spectrum (380–700 nm) of pure water. II. Integrating cavity measurements. *Applied Optics*, **36**, 8710–8723.

PRIEUR, L., and SATHYENDRANATH, S., 1981, An optical classification of coastal and oceanic waters based on the specific spectral absorption curves of phytoplankton pigments, dissolved organic matter and other particulate materials. *Limnology and Oceanography*, **26**, 671–689.

RUNDQUIST, D. C., HAN, L., SCHALLES, J. F., and PEAKE, J. S., 1996, Remote measurement of algal chlorophyll in surface waters: the case for the first derivative of reflectance near 690 nm. *Photogrammetric Engineering and Remote Sensing*, **62**, 195–200.

SATHYENDRANATH, S., PRIEUR, L., and MOREL, A., 1989, A three-component model of ocean colour and its application to remote sensing of phytoplankton pigments in coastal waters. *International Journal of Remote Sensing*, **10**, 1373–1394.

SMITH, R. C., and BAKER, K. S., 1978, Optical classification of natural waters. *Limnology and Oceanography*, **23**, 260–267.

SMITH, R. C., and BAKER, K., 1981, Optical properties of the clearest natural waters. *Applied Optics*, **20**, 177–184.

SPIEGEL, M. R., 1988, *Theory and Problems of Statistics* (New York: McGraw-Hill).

SPITZER, D., and DIRKS, R. W. J., 1987, Bottom influence on the reflectance of the sea. *International Journal of Remote Sensing*, **8**, 279–290.

TASSAN, S., 1998, A procedure to determine the particulate content of shallow water from Thematic Mapper data. *International Journal of Remote Sensing*, **19**, 557–562.

TSAI, F., and PHILPOT, W., 1998, Derivative analysis of hyperspectral data. *Remote Sensing of Environment*, **66**, 41–51.

VAN DE HULST, H. C., 1957, *Light Scattering by Small Particles* (New York: Dover Publications).